Cobalt(II), Nickel(II) and Zinc(II) Coordination Chemistry of the *N*,*N*'-DisubstitutedHydroxylamine-(diamido) Ligand, 3,3′-(Hydroxyazanediyl)dipropanamide

Michael G. Papanikolaou[a], Sofia Hadjithoma[b], Haralampos N. Miras[c,*], Anastasios D. Keramidas[b,*], Themistoklis A. Kabanos[a,*]

[a]*Section of Inorganic and Analytical Chemistry, Department of Chemistry, University of Ioannina, 45110 Ioannina (Greece)*

[b]*Department of Chemistry, University of Cyprus, 2109 Nicosia (Cyprus)*

[c]*WestCHEM, School of Chemistry, University of Glasgow, Glasgow G12 8QQ (UK)*

Dedicated to Professor Spyros Perlepes on the occasion of his 65th birthday

Keywords: Hydroxylamines, NMR, HR-MS, X-ray structure

ABSTRACT

Although directly relevant to metal mediated biological nitrification and the coordination chemistry of peroxide, the transition metal complexes of hydroxylamines and their functionalized variants remain mainly unexplored except vanadium(V) and molybdenum(VI). Reaction of the chelating hydroxylamine ligand 3,3′ -(hydroxyazanediyl)dipropanamide (Hhydia) with$[M^{II}(CH_3COO)_2]\cdot xH_2O$ (M = Co^{II}, Zn^{II}) in methyl alcohol solution yields the complexes $[Co^{II}(\ \eta^1\text{:}\ \eta^1\text{-}CH_3COO)(\ \eta^1\text{-}CH_3COO)(Hhydia)]$, (**1**) and $[Zn^{II}(\eta^1\text{-}CH_3COO)_2(Hhydia)]$,**(4**), while reaction of Hhydia with *trans*-$[Ni^{II}Cl_2(H_2O)_4]\cdot 2H_2O$ yields $[Ni^{II}(Hhydia)_2]Cl_2$(**3**). The X-ray structure analysis of **1** and **4** revealed that the Co^{II} and Zn^{II} atoms are bonded to a neutral tridentate *O*,*N*,*O*-Hhydia ligand and a chelate and a monodentate acetate groups in a severely distorted octahedral geometry for **1** and two monodentate acetate groups for **4** in a highly distorted trigonal bipyramidal geometry (τ = 0. 63). The X-ray structure analysis of **3** revealed that the nickel atom in $[Ni^{II}(Hhydia)_2]^{2+}$ is bonded to two neutral tridentate *O*,*N*,*O*-Hhydia ligands. The twist angle, θ, in $[Ni^{II}(Hhydia)_2]^{2+}$is 55. $1(2)^0$, that is, very close to an ideal octahedron. The metal / Hhydia complexes were studied by UV-vis (cobalt and nickel compounds), NMR (zinc compounds), HR-MS spectroscopy. The ^1H and ^{13}C NMR spectra of the methyl alcohol or acetonitrile solutions of Zn^{II}-Hhydia complexes show the existence of both the 1:1 and 1:2 metal:ligand species being in dynamic equilibrium. The exchange processes between the Zn^{II}-Hhydia is through complete dissociation-association of the ligand from the complexes as it is evident from the 2D $\{^1H\}$ EXSY NMR spectroscopy. UV-vis spectroscopy of the Co^{II}-Hhydia in methyl alcohol also shows the existence of both the 1:1 and 1:2 metal:ligand species in contrast to 1:2 complex $[Ni^{II}(Hhydia)_2]^{2+}$ which is the only species found in solution.. The NMR and UV-vis observations are additionally supported by the HR-MS studies.

1. Introduction

Over the past few years, our group has studied chromium(III) [1], vanadium(V) [2], and molybdenum(VI) [2-5] compounds bearing chelating *N*,*N*′ -disubstituted-(hydroxylamino) ligands, inspired by the naturally occurring non-oxidovanadium(V) compound in mushrooms of the genus Amanita, where the chelating *N*,*N*-disubstituted-(hydroxylamino) ligand *N*-hydroxy-α,α′ -iminodipropionate, hidpa^{3-}, (Scheme 1) binds very tightly to vanadium [6-12]. During the course of this research, it became clear that this kind of ligands give very thermodynamically stable complexes and a very rich chemistry [2-5]. Hydroxylamines have also attracted our attention because they are selective antibacterial agents [13], strong antioxidants [14, 15], drug metabolites [16], and effective metal detoxification [17-22]. In an effort to expand our investigation of interaction of *N*,*N*′ -disubstituted-(hydroxylamino) ligands with transition metal ions, we embarked upon exploring the chemistry of the 3,3′ -(hydroxyazanediyl)dipropanamide (Hhydia) ligand (Scheme 1) with the biologically relevant transition metal ions cobalt(II), nickel(II) and zinc(II). Interestingly, the crystallographically characterized Co^{II}, Ni^{II} and Zn^{II}/hydroxylamine based complexes are very limited [23-28].

.

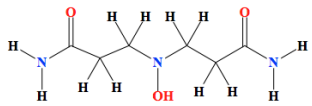

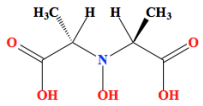

Scheme 1. The *N*,*N*′ -disubstituted(hydroxylamino) ligands Hhydia, and H_3hidpa.

The metal complexes of Co^{II}, Ni^{II} and Zn^{II} with the ligand Hhydia, which incorporates the biological functionalities hydroxylamine and the amide (Scheme 1), might add valuable information into their chemistry. Moreover, the organic molecule Hhydia is an antioxidant and prevents the oxidation of various organic materials even in the presence of oxygen or ozone [29]. It is well-known that antioxidants inhibit oxidation of molecules that are vital for cellular processes and protect the cells from oxidative stress-mediated damage [30-32]. Oxidative stress is a critical component of diseases such as neuronal disease, sickle cell disease, heart malfunction, diabetes, etc. [33-37].

Herein, it is reported the synthesis, structural and physicochemical characterization (UV-vis, HR-MS spectroscopy, and NMR) of the cobalt(II), nickel(II) and zinc(II) complexes with the ligand Hhydia.

2. Experimental

2. 1. Materials

All starting materials were available from commercial suppliers and were used without further purification. All chemicals and solvents were purchased from Sigma–Aldrich. The reactions and all manipulations of the samples were carried out under aerobic conditions. The ligand 3,3′-(Hydroxyazanediyl)dipropanamide (Hhydia) was synthesized according to the literature [1].

2. 2. Preparations

2. 2. 1. ***Preparation of* [(η^1: η^1-acetato)(η^1-acetato)[3,3′-(hydroxyazanediyl)dipropanamide-*O,N,O*]cobalt(II), [Co^{II}(η^1: η^1-CH_3COO)(η^1-CH_3COO)(Hhydia)]· H_2O, (1· H_2O).** To a stirred methyl alcohol (5 ml) solution of $[Co^{II}(CH_3COO)_2]\cdot 4H_2O$ (142 mg, 0. 57 mmol, 1.0 equiv) was added solid Hhydia (100 mg, 0. 57 mmol, 1.0 equiv) in one portion. Upon addition of the ligand

the pink color of the solution changed to purple. The solution was stirred for an additional hour, after which its volume was reduced to 2 ml then diethyl ether (15 ml) was added to the solution dropwise and a purple solid was formed. The solid was filtered, washed with 5 ml of diethyl ether and dried in vacuo. Yield: (143 mg, 0.39 mmol 68% based on Hhydia). Anal. Calc. (%) for $C_{10}H_{21}N_3O_8Co$ (M_r = 370. 14) C, 32. 41; H, 5. 71; N: 11. 35. Found (%): C, 32. 39; H, 5. 67; N: 11. 32. IR (KBr, cm^{-1}): 3350 (w), 3314 (w), 1656 (s), 1546 (s), 1402 (s), 1083 (w), 916 (w). μ_{eff} = 5. 0 μ_B at 298 K.

Crystals of the cobalt(II) complex **1**· CH_3OH suitable for X-ray diffraction analysis were obtained by layering diethyl ether into a concentrated methyl alcohol solution of **1**· H_2O.

2. 2. 2. ***Preparation of*** **[Co^{II}(Hhydia)Cl_2], 2.** A similar procedure was used as described for **1**· H_2O. Instead of [$Co^{II}(CH_3COO)_2$]· $4H_2O$, $CoCl_2$· $6H_2O$ (136 mg, 0.57 mmol, 1.0equiv) was used. Complex **2** was obtained as a blue-purple solid (125 mg, 0.41mmol, 72%). Anal. Calc. (%) for $C_6H_{13}Cl_2N_3O_3Co$ **(**M_r = 304. 96) C, 23. 61; H, 4. 29; N: 13. 78. Found (%): C, 23. 69; H, 4. 27; N: 13. 42. IR (KBr, cm^{-1}):3500 (w), 3260 (w), 1645 (s), 1575 (s), 893 (w). μ_{eff} = 5. 1 μ_B at 298 K.

2. 2. 3. ***Preparation of*** **Bis-[3,3′-(hydroxyazanediyl)dipropanamide-*O,N,O*]nickel(II) Chloride, [Ni^{II}(Hhydia)$_2$]Cl_2·H_2O, 3·H_2O.** A similar procedure was used as described for **1**· CH_3OH, except that i) instead of [$Co^{II}(CH_3COO)_2$]· $4H_2O$, *trans*-[$Ni^{II}Cl_2(H_2O)_4$]· $2H_2O$ (136 mg, 0.57 mmol, 1.0equiv) and ii) Hhydia (200 mg, 1.14 mmol, 2.0equiv) were used. Complex **3**·H_2O was obtained as a light blue solid (184 mg, 0.37mmol, 65%). Anal. Calc. (%) for $C_{12}H_{28}Cl_2N_6O_7Ni$ (M_r= 497. 85) C, 28. 92; H, 5. 67; N: 16. 84. Found (%): C, 28. 65; H, 5. 35; N: 16. 69. IR (KBr, cm^{-1}): 3252 (w), 3093 (w), 1656 (s), 1595 (s), 897 (m). μ_{eff} = 3. 2μ_B at 298 K.

Crystals of the nickel(II) complex **3**· $1.5H_2O$ suitable for X-ray diffraction analysis were obtained by layering diethyl ether into a concentrated acetonitrile solution of **3**·H_2O.

***2. 2. 4. Preparation of* Bis-(η^1-acetato)[3,3′-(hydroxyazanediyl)dipropanamide-*O,N,O*]zinc(II), [Zn^{II}(η^1-$CH_3COO)_2$(Hhydia)], 4.** To a stirred methyl alcohol solution (5 ml) of $Zn^{II}(CH_3COO)_2 \cdot 2H_2O$ (125 mg, 0.57 mmol, 1.0equiv) was added solid Hhydia (100 mg, 0.57 mmol, 1.0equiv) in one portion. The color of the solution remained colorless and after approximately 15 min a white precipitate was formed. The mixture was stirred for an additional hour; the white solid was filtered, washed with 5 ml of diethyl ether and dried in vacuo. Yield: (170 mg, 0.47 mmol, 83%). Anal. Calc. (%) for $C_{10}H_{19}N_3O_7Zn$ (*M*r = 358. 57) C, 33. 47; H, 5. 31; N: 11. 71. Found (%): C, 33. 35; H, 5. 44; N: 11. 94. IR (KBr, cm^{-1}):3387, (w), 3186 (w), 1645 (s), 1579 (s), 896 (w), 3390 (w), 3197 (w), 1656 (s), 1571 (s), 1402 (s), 900 (w).

Crystals of the zinc(II) complex **4**· CH_3OH suitable for X-ray diffraction analysis were obtained by layering diethyl ether into a concentrated methyl alcohol solution of **4**.

2. 2. 5. ***Preparation of* Zn(Hhydia)Cl_2 (5).** A similar procedure was used as described for **4**. Instead of $Zn^{II}(CH_3COO)_2 \cdot 2H_2O$, $Zn^{II}Cl_2$ (78 mg, 0.57 mmol, 1.0equiv) was used. Complex **6** was obtained as a white solid (136 mg, 0.44mmol, 77%). Anal. Calc. (%) for $C_6H_{13}Cl_2N_3O_3Zn$ (*M*r = 311. 42) C, 23. 12; H, 4. 21; N: 13. 49. Found (%): C, 23. 58; H, 4. 10; N: 13. 48. IR (KBr, cm^{-1}): 3387, (w), 3186 (w), 1645 (s), 1579 (s), 896 (w).

2. 3. Crystal data collection and refinement

Suitable single crystal was selected and mounted onto a rubber loop using Fomblin oil. Single-crystal X-ray diffraction data of **1**·CH_3OH, **3**·$1.5H_2O$ and **4**·CH_3OH were recorded on a Bruker Apex CCD diffractometer ($\lambda(MoK_\alpha)$ = 0.71073 Å) at 150 K equipped with a graphite

monochromator. Structure solution and refinement were carried out with SHELXS-97 [38] and SHELXL-97 [14] usingtheWinGXsoftware package [39]. Data collection and reduction were performed using the Apex2 software package. Corrections for incident and diffracted beam absorption effects were applied using empirical absorption corrections [40]. All non–hydrogen atoms (including those disordered) were refined anisotropically. Solvent water molecule sites with partial occupancy were found and included in the refinement of the structure were generally refined with anisotropic thermal parameters. The positions of hydrogen atoms were calculated based on stereochemical considerations and kept fixed isotropic during refinement. Final unit cell data and refinement statistics for compounds **1**· CH_3OH, **3**· $1.5H_2O$ and **4**· CH_3OH are listed in Table 1.

2. 4. NMR measurements

All NMR samples were prepared by direct dissolution of the zinc(II) compound **4** in CD_3CN-d_3 or MeOD-d_4 at room temperature just prior to the NMR spectrometric determinations. NMR spectra were recorded on a BrukerAvance III 500 MHz spectrometer. A 30º-pulse width was applied for both the ^1H and ^{13}C NMR measurements, 1 s and 2 s relaxation delay, respectively. The standard NOESY pulse sequence (90°-t_1-90°-t_m-90°) was applied in the 2D {^1H} EXSY-NOESY measurements, and these spectra were acquired using 128 increments (with 16 scans each) covering 6 ppm in both dimensions and 0.30 and 0.35 s mixing times (t_m). 2D {^1H, ^{13}C} HSQC spectra were obtained by using standard pulse sequences of Bruker Topspin 3.0 software. These spectra were acquired using, 2D {^1H, ^{13}C} HSQC 128 increments (with 16 scans each) covering 100 and 6 ppm at F1 and F2 dimensions respectively.

2. 5. ESI-MS measurements

Electrospray ionization mass spectrometry was performed using a Bruker micrOTOF-Q quadrupole time-of-flight mass spectrometer. Samples were dissolved in water and CH_3OH introduced at a dry gas temperature of 180 °C. The calibration solution used was Agilent ES tuning mix solution, enabling calibration between approximately 100m/z and 3000m/z. This solution was diluted 60:1 with acetonitrile. Samples were introduced into the MS *via* direct injection at 180 μL/h. The ion polarity for all MS scans recorded was positive, with the voltage of the capillary tip set at +4000 V, end plate offset at -500 V, funnel 1 RF at 400 Vpp and hexapole RF at 200 Vpp, ion energy 5.0 eV, collision energy at 10 eV, collision cell RF at 1000 Vpp, transfer time at 120.0 μs, the pre-pulse storage time at 10.0 μs. The collected data were analysed using the Bruker Daltonics v4.1 software whilst simulated isotope patterns were investigated using Bruker isotope pattern software.

2. 6. Details of instrumentation

Elemental analyses (carbon, hydrogen and nitrogen) were performed using a Perkin Elmer 240C elemental analyzer. Fourier-transform infrared (FTIR) spectra of the various compounds dispersed in KBr pellets were recorded in a transmittance configuration using a Bruker spectrometer (Alpha model). Electronic absorption spectra were measured as solutions in septum-sealed quartz cuvettes on a Jasco V570/UV/Vis/NIR spectrophotometer.

3. Results and discussion

3. 1. Synthesis

The cobalt(II), nickel(II) and zinc(II) complexes with the ligand Hhydia were synthesized according to Scheme 2. When the metal(II) source was the chloride salt, reaction of it with

Hhydia in a molar ratio 1:1 resulted in the isolation of compounds **2**·H_2O, **3**·H_2O and **5,** while in the case of the molar ratio of 1:2 [$M^{II}Cl_2$: Hhydia] complex **3**·H_2O, in much higher yield, and **5** were isolated, but not the complexes $[Co^{II}(Hhydia)_2]^{2+}$ and $[Zn^{II}(Hhydia)_2]^{2+}$. UV-vis, NMR and HR-MS measurements (vide infra) reveal that in methyl alcohol solution the complexes $[Co^{II}(Hhydia)_2]^{2+}$ and $[Zn^{II}(Hhydia)_2]^{2+}$ are present, but are hydrolytically unstable; in marked contrast the $[Ni^{II}(Hhydia)_2]^{2+}$ complex is the most thermodynamically stable species. When the metal source was $[M^{II}(CH_3COO)_2]$ we succeeded the isolation of the compounds **1**·H_2O and **4** only irrespective of the molar ratio of $[M^{II}(CH_3COO)_2]$:Hhydia.

Efforts to isolate complexes of Co^{II} /Ni^{II} / Zn^{II} with the deprotonated hydroxylamine group of Hhydia by reacting the acetate salts of Co^{II}, Ni^{II}, and Zn^{II} in refluxing methyl alcohol were unsuccessful. The synthesis of copper(II) complexes with Hhydia failed because presumably there is a redox reaction between the copper(II) and the hydroxylamine group.

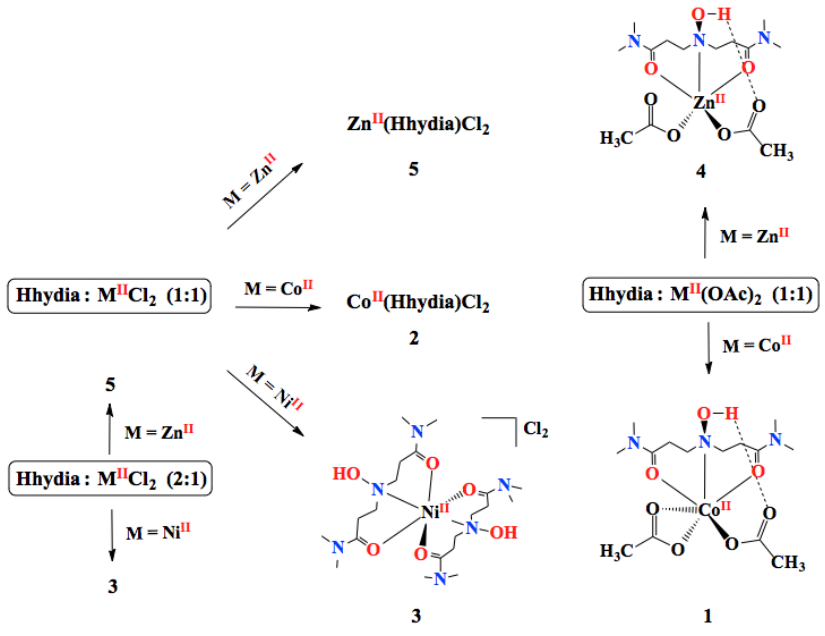

Scheme 2. Synthesis of the complexes **1**·H_2O-**5**.

3. 2. Description of the structures

*3. 2. 1. [Co^{II}(η^1: η^1-CH_3COO)(η^1-CH_3COO)(Hhydia)]· H_2O, **1**· H_2O*

The molecular structure of the neutral cobalt(II) compound **1**· $CH_3OH$is shown in Figure 1. A selection of interatomic distances and bond angles relevant to the coordination sphere of cobalt(II) is listed in Table 2. The cobalt(II) atom in **1** is bonded to a neutral tridentate (*O*,*N*,*O*) Hhydia ligand, to a symmetric chelating and a unidentate acetate groups. The donor atoms surrounding the cobalt ion are disposed in a severely distorted octahedral geometry where the two carbonyl oxygen atoms occupy the axial positions and the hydroxylamine nitrogen atom and the three acetate oxygen atoms occupy the equatorial plane. The Hhydia ligand forms two six-membered fused chelate rings with the cobalt(II) center. The average Co^{II}–O_{amide} bond length [2.072(2) Å] is much longer (≈ 0.12Å) in comparison to the Cr^{III}–O_{amide} bond length in the only one reported metal complex of Hhydia, $[Cr^{III}(Hhydia)_2]^{3+}$, while the ($Co^{II}$–$N_{hydroxylamine}$) bond length [2.147(2) Å] is slightly longer (≈ 0.03 Å) in comparison to $[Cr^{III}(Hhydia)_2]^{3+}$. The longer bond distances of Hhydia to cobalt(II) are presumably due to its lower oxidation state. There is an intramolecular hydrogen bond in **1**· CH_3OH between the hydrogen atom attached to the $O_{hydroxylamine}$ and the free oxygen atom of the monodentate acetate group (Figure 1).

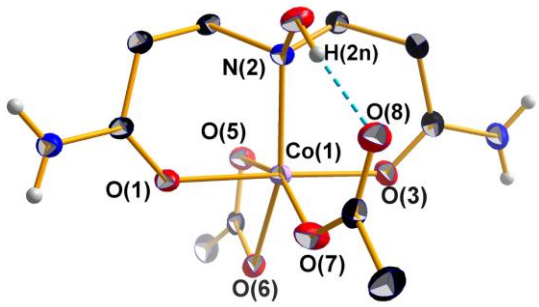

Figure 1. ORTEP diagram of **1**· CH_3OH with atomic numbering scheme and thermal ellipsoids at 50% probability level. The methylene and methyl hydrogen atoms and crystal lattice CH_3OH molecules were omitted for clarity.

*3.2.2. [$Zn^{II}(\eta^1$-$CH_3COO)_2(Hhydia)$]· CH_3OH, **4**· CH_3OH*

The molecular structure of the neutral zinc(II) compound **4**· $CH_3OH$is shown in Figure 2. A selection of interatomic distances and bond angles relevant to the coordination sphere of zinc(II) is listed in Table 2. The zinc(II) atom in **4** is bonded to a neutral tridentate (*O*, *N*, *O*) Hhydia ligand, to two unidentate acetate ligands. The donor atoms surrounding the zinc(II) ion are disposed in a severely distorted trigonal bipyramidal geometry, τ = 0.63[41], where the two carbonyl oxygen atoms occupy the axial positions and the hydroxylamine nitrogen atom and the two acetate oxygen atoms occupy the equatorial plane. The Zn^{II}–$N_{hydroxylamine}$ bond length [2.142(2) Å] is almost identical to the Co^{II}–$N_{hydroxylamine}$ bond length [2.147(2) Å] in **1**· CH_3OH, while the average $d(Zn^{II}–O_{amide})$ 2.099(2)Å is 0.027 Å longer in comparison to mean $d(Co^{II}–O_{amide})$in **1**·CH_3OH.

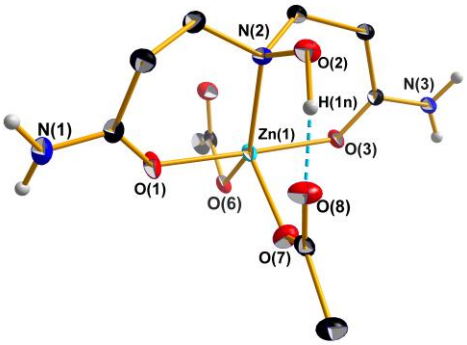

Figure 2. ORTEP diagram of **4**· CH_3OH with atomic numbering scheme and thermal ellipsoids at 50% probability level. The methylene and methyl hydrogen atoms and crystal lattice CH_3OH molecules were omitted for clarity.

3.2 3. $[Ni^{II}(Hhydia)_2]Cl_2{\cdot}1.5H_2O$, ***3***$\cdot 1.5H_2O$

. The molecular structure of the cation $[Ni^{II}(Hhydia)_2]^{2+}$ is shown in Figure 3. A selection of interatomic distances and bond angles is listed in Table 3. The nickel(II) atom in $[Ni^{II}(Hhydia)_2]^{2+}$ is bonded to two neutral tridentate Hhydia ligands, and each of the two Hhydia ligands acts as a tridentate *O*, *N*, *O* donor (Figure 3). The nickel(II) atom is an inversion center in the cation $[Ni^{II}(Hhydia)_2]^{2+}$. The donor atoms surrounding the nickel(II) atom are disposed in an octahedral geometry where four carbonyl oxygen atoms of two different ligand molecules occupy the equatorial plane, and the two *trans*-hydroxylamine nitrogen atoms occupy the axial positions. The twist angle (θ) [42] in $[Ni^{II}(Hhydia)_2]^{2+}$is $55.1(2)^0$, which is, very close to ideal octahedron. The four amide functionalities are planar within the limits of precision. Each of the two Hhydia ligands forms two six-membered fused chelate rings and is meridionally ligated to the nickel(II) atom. The two planes defined by the three donor atoms (*O*, *N*, *O*) of each ligand are found to be perpendicular to one another with adihedral angle of $89.6(1)^0$. The $d[Ni^{II}\text{-}N_{hydroxylamine}]$ = 2.093(2)Å and mean $d[Ni^{II}\text{-}O_{amide}]$ = 2.030(2)Å are shorter by ≈ 0.05 Å in

comparison to corresponding bond lengths in **1**· CH_3OH and **4**· CH_3OH and this might explain its thermodynamic stability (vide infra).

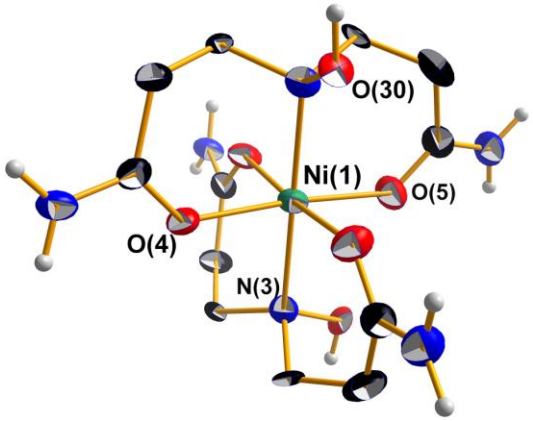

Figure 3. ORTEP diagram of $[Ni^{II}(Hhydia)_2]^{2+}$ with atomic numbering scheme and thermal ellipsoids at 50% probability level. The methylene hydrogen atoms, Cl^- counter ions, and crystal lattice H_2O molecules were omitted for clarity.

3.3. UV-vis spectroscopy

In Table 4 are summarized the UV-vis spectral data of the complexes **1**· H_2O, **2** and **3**· H_2O. In addition, the spectral changes of **1**· H_2O, and **2** after the addition of Hhydia are also reported. Compounds **1**· H_2O, and **2** in methyl alcohol gave one broad peak (Figure 4) which was assigned to the transitions $^4T_{1g} \leftarrow {}^4T_{1g}(P)$ (531 nm) and $^4A_{2g} \leftarrow {}^4T_{1g}$ (481 nm) in accordance with an octahedral high spin $Co^{II}(d^7)$ system. Addition of Hhydia to the methyl alcohol solutions of **1**· H_2O, and **2** resulted to a blue shift of the peaks at 531 and 481 nm, to 509 and 475 nm respectively, which is consistent with the formation of $[Co^{II}(Hhydia)_2]^{2+}$ complex, with a N_2O_4 coordination sphere, while the complex $[Co^{II}(Hhydia)(CH_3OH)_3]^{2+}$ has a NO_5 coordination sphere. The intensity of the band assigned to the $[Co^{II}(Hhydia)_2]^{2+}$ complex increases even after the addition of 4 equivalents of Hhydia (Figure 4) indicative of the complex's hydrolytic instability.

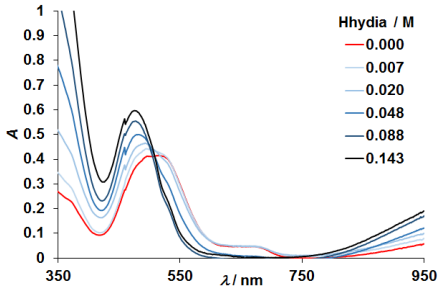

Figure 4: UV-vis spectra of methyl alcohol solutions containing complex **2** (0.0394 M) and various concentrations of Hhydia.

The UV-vis spectrum of the nickel(II) complex **3**·H_2O in methyl alcohol gave three peaks at 363, 591 and 924 nm (Figure 5) as expected for an octahedral Ni^{II} (d^8) system, and were assigned to transitions $^3T_{2g}(P) \leftarrow {}^3A_{2g}$, $^3T_{2g} \leftarrow {}^3A_{2g}$ and $^3T_{2g} \leftarrow {}^3A_{2g}$ respectively. Addition of the ligand Hhydia to the methyl alcohol solution of **3**· H_2O did not affect the features of the initial spectrum apart from a slight increase of the band's which means that in solution the major Ni^{II} species is the $[Ni^{II}(Hhydia)_2]^{2+}$.

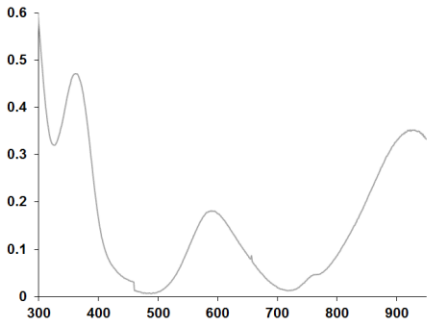

Figure 5. UV-vis spectrum of complex **3**· H_2O (0.0307 g/2mL) in CH_3OH.

3. 4. NMR spectroscopy

The ^{1}H and ^{13}C NMR spectra of the two Zn^{II} compounds **4** and **5** in CD_3OD-d_4 gave broad peaks, due to the fast exchange between the Zn^{II} - Hhydia species in the solution (Figure S1). The ^{13}C NMR spectrum of complex **4** in CD_3OD-d_4 showed a shift for the peaks of the carbonyl carbon atoms by 2.2 ppm shift to a weaker field in comparison to the free ligand, and is indicative of coordination of the carboxyl oxygen atoms of Hhydia (Table 5) to the Zn^{II}. The ^{1}H NMR spectrum of **5** in CD_3OD-d_4 was very similar to that of **4**, except that the spectrum of **4** has an additional sharp peak for the acetate moiety with a chemical shift at 1.99 ppm, which is very close to the peak of free acetate (1.96 ppm) which is clear that the CH_3COO^- group in solution is not bound to the Zn^{II}. The 2D $\{^{1}H,^{13}C\}$ grHMQC spectrum of complex **4** (Figure S2) in CD_3OD-d_4 gave three peaks for each carbon atom of Hhydia (see Scheme 3 for numbering), indicating the presence of three Hhydia species in the solution, i.e., the free Hhydia, and the zinc(II)/Hhydia complexes $[Zn^{II}(Hhydia)(CH_3OH)_2]^{2+}$ (**6**) and $[Zn^{II}(Hhydia)_2]^{2+}$ (**7**). Addition of 1 equivalent of ligand Hhydia to the CD_3OD solution of **4** increases the intensity of the peaks associated with Hhydia and $[Zn^{II}(Hhydia)_2]^{2+}$ and become broader, making difficult to be distinguished. The 2D $\{^{1}H\}$ grEXSY spectrum of **4** in CD_3OD-d_4 (Figure 6) gave off diagonal peaks between the ^{1}H NMR resonances of Hhydia, **6**, and **7** and this fact reveals two intermolecular exchange processes between the couples Hhydia / **6** and **6** / **7** (Scheme 3). The ^{1}H NMR spectrum of **4** in CD_3CN-d_3 is similar to that in CD_3OD, except the presence of two peaks due to the inequivalent amide protons, $-C(=O)NH_aH_b$. The H_a shows an exchange with H_b in the 2D $\{^{1}H\}$ grEXSY spectrum (Figure S3) probably through the fast intermolecular exchange mechanism of the labile Zn^{II}-Hhydia species shown in Scheme 3.

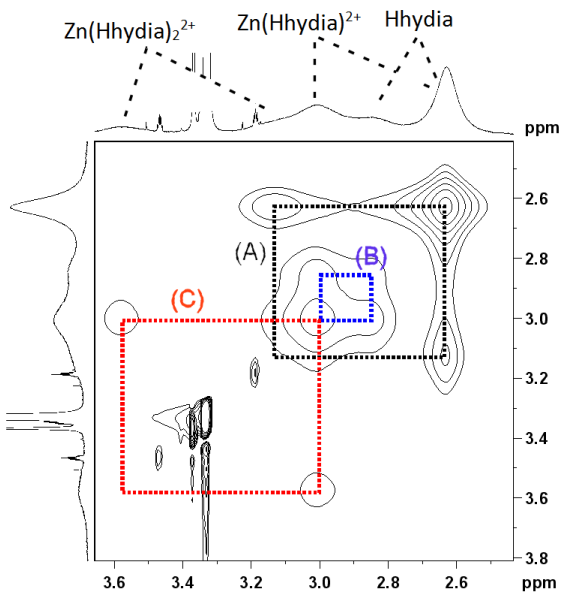

Figure 6. 2D {^{1}H} grEXSY spectrum of compound **4** (*C* = 5.0 mM) in CD_3OD, t_m=300 ms.

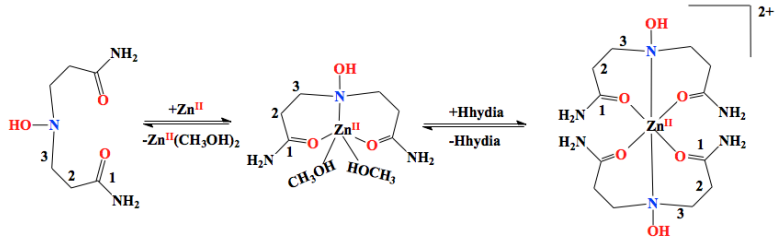

Scheme 3. Exchange mechanism between the couples Hhydia / **6** and **6** / **7**

3. 5. ESI-MS

Given the evidence of hydrolytic instability of the [M^{II}(Hhydia)X_2] complexes (M = Co^{II}, Zn^{II} and X = Cl^-, CH_3COO^-) obtained from the UV-vis (for Co^{II}) and NMR (for Zn^{II}) spectroscopies, we embarked on an effort to investigate further the behaviour of the reported complexes in solution and monitor the *in-situ* conversion of 1:1 towards the formation of 1:2 complexes upon addition of one equivalent of ligandusing high resolution electrospray ionization mass spectrometry.

A real time comparative study was carried out using preformed $[M^{II}(Hhydia)X_2]$ complexes dissolved in methyl alcohol solution. The first observations show that the X group which completes the coordination sphere of the transition metal affects the hydrolytic stability of the complexes and their subsequent transformation to 1:2 complexes. More specifically,the $[M^{II}(Hhydia)Cl_2]$ type of complexes seem to retain their integrity duringthe course of the ESI-MS studies as evidenced in Figure 7. The observed distributionenvelopes were assigned to the singly charged species$\{[Zn^{II}(Hhydia)Cl]\}^+$, and $\{[Co^{II}(Hhydia)Cl]\}^+$centered at *m/z* ca. 273.99, and 268.99 respectively. Upon addition of one equivalent of ligand Hhydia into the same solution of $[M^{II}(Hhydia)Cl_2]$ complexes, we observed instantly the generation of 1:2 complexes as evidenced by a series of distribution envelopes for $\{[Zn^{II}(Hhydia)(hydia)]\}^+$, and $\{[Co^{II}(Hhydia)(hydia)]\}^+$ centered at *m/z* ca. 413.10 and 408.11 respectively. It is worth noting that when the $[M^{II}(Hhydia)(CH_3COO)_2]$ complexes were used as starting point, an instant conversion to the 1:2 complexes took place upon addition of one equivalent of Hhydia. There is a clear indication that the acetate groups can be replaced by Hhydia ligands much easier (see NMR discussion) and can not prevent their conversion to the 1:2 aducts. It is worth noting that the deprotonation of the hydroxylamine proton took place in some species during the course of the ESI-MS studies. This type of phenomena such as change of the redox state of thetransition metal center and gain or loss of protons and/orsolvent molecules is a quite common effect that takes place during the ionization process and has beenobserved before [43-48].

Complex **3**·H_2O i. e. , $[Ni^{II}(Hhydia)_2]Cl_2\cdot H_2O$ gave three distribution envelopes which were assigned to the singly charged species $[Ni^{II}(Hhydia)Cl]^+$, $[Ni^{II}(Hhydia)(hydia)]^+$ and $[Ni^{II}(Hhydia)_2Cl]^+$ centered at *m/z* ca. 267.99, 407.11, and 443.09 respectively. Upon addition

of one equivalent of Hhydia to the solution of **3**·H_2O the distribution envelope corresponding to the 1:2 adduct found to be more pronounced (Figure 7 c/c').

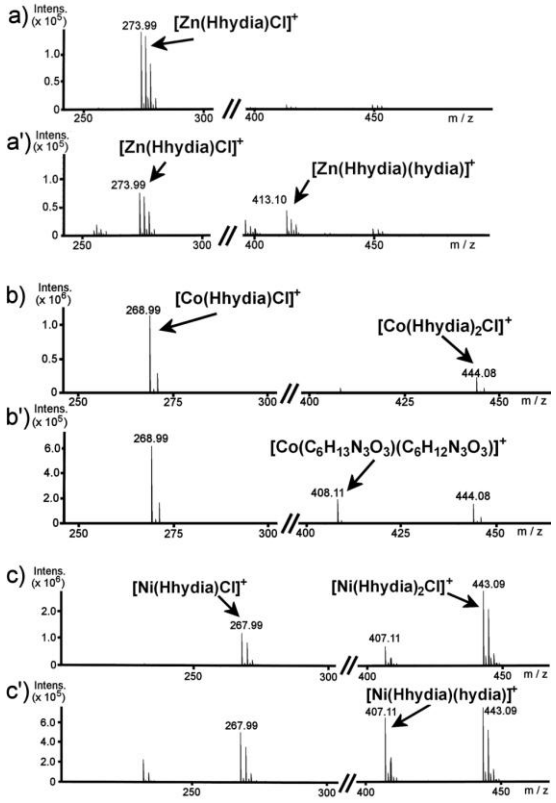

Figure 7. ESI-MS of [M^{II}(Hhydia)X_2] complexes (Where M: Co^{II}, $Zn^{II}$and X: Cl^-) in methyl alcohol solution in the absence (A) and presence of one equivalent of Hhydia(A') respectively. A: [[Zn^{II}(Hhydia)Cl_2]; B: [[Co^{II}(Hhydia)Cl_2] and C: [Ni^{II}(Hhydia)$_2$]Cl_2.

4. Conclusion

In conclusion, stable hydroxylamine complexes of transition metals cobalt(II), nickel(II), and zinc(II) were synthesized through chelation reactions. The neutral *N,N′* -disubstituted-(hydroxylamino) chelating ligand Hhydia binds to the three metals through the two carbonyl oxygen atoms and the hydroxylamine nitrogen atomforming two six-membered fused chelate rings with them. The ^1H and ^{13}C NMR spectra of Zn^{II}-Hhydia complexes in methyl alcohol reveal the existence of both the 1:1 and 1:2 metal:ligand species being in dynamic equilibrium.

UV-vis spectroscopy of the Co^{II}-Hhydia complexes in methyl alcohol also shows the existence of both the 1:1 and 1:2 metal:ligand species in contrast to 1:2 complex $[Ni^{II}(Hhydia)_2]^{2+}$which is the only species found in solution. Moreover, the NMR and UV-vis observations are nicely supported by the X-Ray single crystal measurements.

The X-ray structural analysis of the complexes **1**, **3**, and **4** provides evidence in solid state that the $M^{II}–O_{amide}$ and M^{II}-$N_{hydroxylamine}$ binding are possible modes of interaction of Co^{II}, Ni^{II}, and Zn^{II} in biological systems. Solution studies also support these binding modes.

Corresponding Authors

*Themistoklis A. Kabanos, E.Mail: tkampano@cc.uoi.gr.

*Anastasios D. Keramidas, E.Mail: akeramid@ucy.ac.cy.

*Haralampos N. Miras, E.Mail: Charalampos.Moiras@glasgow.ac.uk

ORCID

Themistoklis A. Kabanos: 0000-0003-4336-6128

Anastasios D. Keramidas: 0000-0002-0446-8220

Haralampos N. Miras: 0000-0002-0086-5173

Acknowledgements

The authors wish to thank Assistant Professor Dr. Angelos G. Kalampounias, Department of Chemistry, University of Ioannina for helping in recording FTIR spectra.

Appendix A. Supplementary data

The crystallographic data for compounds **1**·CH_3OH, **3**·$1.5H_2O$and **4**·CH_3OH with CCDC numbers 1831952, 1831953, and 1831954 respectively, can be obtained free of charge from the Cambridge Crystallographic Data Centre, 12, Union Road, Cambridge CB2 1EZ; fax: (+44)

1223- 336-033, deposit@ccdc. cam. ac. uk. Supplementary data (Figures S1-S3) associated with this article can be found, in the online version, at……

Table 1.

Crystal data and refinement details for complexes **1**· CH_3OH, **3**· $1.5H_2O$ and **4**· CH_3OH

Complex	**1**· CH_3OH	**3**· $1.5H_2O$	**4** · CH_3OH
Formula	$C_{11}H_{22}CoN_3O_8$	$C_{24}H_{41}Cl_4N_{12}Ni_2O_{16}$	$C_{11}H_{19}N_3O_8Zn$
Formula Weight	383.25	1012.91	386.66
Crystal System	Monoclinic	Monoclinic	Monoclinic
Space group	P 21/n	P 2/n	P 21/n
a(Å)	7.6607(5)	15.746(7)	7.5973(4)
b(Å)	24.3439(14)	15.621(7)	24.2334
c(Å)	9.3186(7)	18.730(8)	9.4716(6)
a (^{o})	90	90	90
β (^{o})	109.969(8)	105.839(6)	110.459(6)
γ (^{o})	90	90	90
D_{calc}[Mg/m^3]	1.558	1.518	1.572
μ [mm^{-1}]	1.094	1.165	1.547
F(000)	800	2084	800
Total reflections	9544	46669	10141
Unique reflections	3877	9149	3926
Observed Data [I > 2 σ(I)]	3877	9149	3926
No of parameters	210	638	224
R_{int}	0.0357	0.1298	0.0366
R_1, wR_2 (all data)	0.0444, 0.1109	0.1719, 0.2151	0.0472, 0.1175
R_1, wR_2 [I > 2 σ(I)]	0.0586, 0.1209	0.0725, 0.1644	0.0452, 0.1163

Table 2.

Selected bond lengths (Å) and angles (°) of complexes **1**·CH_3OH and **4**·CH_3OH.

Complex	**1**·CH3OH	**4**·CH3OH
N(2) - M[a]	2.147(2)	2.142(2)
O(1) - M	2.0780(19)	2.081(2)
O(3) - M	2.066(2)	2.1170(19)
O(5) - M	2.198(2)	-
O(6) - M	2.170(2)	2.047(2)
O(7) - M	2.010(2)	1.978(2)
O(7) - M - O(3)	92.41(9)	88.60(9)
O(7) - M - O(1)	87.79(9)	93.50(9)
O(3) - M - O(1)	177.64(8)	177.82(9)
O(7) - M - N(2)	109.25(9)	117.90(9)
O(3) - M - N(2)	92.12(8)	88.08(8)
O(1) - M - N(2)	90.04(8)	91.45(9)
O(7) - M - O(6)	98.20(8)	101.35(8)
O(3) - M - O(6)	91.69(8)	86.68(8)
O(1) - M - O(6)	85.96(8)	92.32(8)
N(2) - M - O(6)	152.08(8)	140.24(8)
O(7) - M - O(5)	157.99(8)	-
O(3) - M - O(5)	89.91(8)	-
O(1) - M - O(5)	89.03(8)	-
N(2) - M - O(5)	92.51(8)	-
O(6) - M - O(5)	59.85(8)	-

[a]M corresponds to Co(1) and Zn(1) for **1**·CH3OH and **4**·CH3OH respectively.

Table 3.

Selected bond lengths (Å) and angles (°) of complex **3**· 1.5H_2O

Complex	**3**· 1.5H_2O
N(2)/N(2)'–Ni(1)	2. 093(2)
O(1)/O(1)' – Ni(1)	2.028(2)
O(3)/O(3)' – Ni(1)	2.032(2)
N(2) - Ni(1) - O(1)	92.3(9)
N(2) - Ni(1) - O(1)'	93.79(9)
N(2) - Ni(1) - O(3)	87.6(8)
N(2) - Ni(1) - O(3)'	87.0(9)
N(2) - Ni(1) - N(2)'	180.0(2)
O(1) - Ni(1) - O(3)	174.6(8)
O(1) - Ni(1) - O(3)'	87.5(8)
O(1) - Ni(1) - O(1)'	92.9(8)

Table 4.

UV-vis spectral data for **1**· H_2O, **2**, and **3**· H_2O.

Complex	**10Dq**[a] **(B)**[a]	λ^b **(ε)**[c]
1· H_2O	11000 (550)	531 (7.6)
		481 (7.2)
1· H_2O +Hhydia[d]	11100 (654)	509 (8.3)
		475 (7.8)
2	10900 (574)	530 (7.6)
		480 (8.0)
2+ Hhydia[d]	11000 (610)	509 (8.3)
		475 (7.8)
3· H_2O	10800 (750)	363 (15.4)
		591 (6.0)
		924 (11.6)

[a]In cm^{-1}. [b] In nm. [c] In $cm^{-1}M^{-1}$. [d] Various quantities of Hhydia were added to the CH_3OH solution of **1**· H_2O and **2** (Figure 4).

Table 5.

^{13}C (^{1}H) chemical shifts (ppm) of Hhydia, **6**, and **7** which are formed upon dissolution of **4** in CD_3OD

	Hhydia	**6**	**7**
C1[a]	177.2	179.4	179.4
C2[a]	28.4 (2.626)	31.4 (2.626)	32.7 (3.127)
C3[a]	56.5 (2.829)	56.5 (3.014)	56.5 (3.581)

[a] The numbering is shown in Scheme 3.

References

[1] P.A. Tziouris, C.G. Tsiafoulis, M. Vlasiou, H.N. Miras, M.P. Sigalas, A.D. Keramidas, T.A. Kabanos, Interaction of Chromium(III) with a N, N ′-disubstituted hydroxylamine-(diamido) ligand: A combined experimental and theoretical study, Inorganic Chemistry, 53 (2014) 11404-11414.

[2] V.A. Nikolakis, J.T. Tsalavoutis, M. Stylianou, E. Evgeniou, T. Jakusch, A. Melman, M.P. Sigalas, T. Kiss, A.D. Keramidas, T.A. Kabanos, Vanadium(V) compounds with the bis-(hydroxylamino)-1,3,5-triazine ligand, H2bihyat: Synthetic, structural, and physical studies of [V 2VO3(bihyat)2] and of the enhanced hydrolytic stability species cis-[VVO2(bihyat)], Inorganic Chemistry, 47 (2008) 11698-11710.

[3] V.A. Nikolakis, V. Exarchou, T. Jakusch, J.D. Woolins, A.M.Z. Slawin, T. Kiss, T.A. Kabanos, Tris-(hydroxyamino)triazines: High-affinity chelating tridentate O,N,O-hydroxylamine ligand for the cis-VVO2+ cation, Dalton Transactions, 39 (2010) 9032-9038.

[4] V.A. Nikolakis, P. Stathopoulos, V. Exarchou, J.K. Gallos, M. Kubicki, T.A. Kabanos, Unexpected synthesis of an unsymmetrical μ-oxido divanadium(V) compound through a reductive cleavage of a N-O bond and cleavage-hydrolysis of a C-N bond of an N,N-disubstituted Bis-(hydroxylamino) ligand, Inorganic Chemistry, 49 (2010) 52-61.

[5] M. Stylianou, V.A. Nikolakis, G.I. Chilas, T. Jakusch, T. Vaimakis, T. Kiss, M.P. Sigalas, A.D. Keramidas, T.A. Kabanos, Molybdenum(VI) coordination chemistry of the N,N-disubstituted bis(hydroxylamido)-1,3,5-triazine ligand, H2bihyat. Water-assisted activation of the MoVI=O bond and reversible dimerization of cis-[MoVIO2(bihyat)] to [MoVI2O 4(bihyat)2(H2O)2], Inorganic Chemistry, 51 (2012) 13138-13147.

[6] D. Rehder, Bioinorganic vanadium chemistry, 2008.

[7] C. Li, N.H. Oberlies, The most widely recognized mushroom: Chemistry of the genus Amanita, Life Sciences, 78 (2005) 532-538.

[8] C.D. Garner, E.M. Armstrong, R.E. Berry, R.L. Beddoes, D. Collison, J.J.A. Cooney, S.N. Ertok, M. Helliwell, Investigations of Amavadin, Journal of Inorganic Biochemistry, 80 (2000) 17-20.

[9] E.M. Armstrong, D. Collison, N. Ertok, C.D. Garner, NMR studies on natural and synthetic Amavadin, Talanta, 53 (2000) 75-87.

[10] R.E. Berry, E.M. Armstrong, R.L. Beddoes, D. Collison, S.N. Ertok, M. Helliwell, C.D. Garner, The structural characterization of amavadin, Angewandte Chemie - International Edition, 38 (1999) 795-797.

[11] P.D. Smith, R.E. Berry, S.M. Harben, R.L. Beddoes, M. Helliwell, D. Collison, C.D. Garner, New vanadium-(IV) and -(V) analogues of Amavadin, Journal of the Chemical Society - Dalton Transactions, (1997) 4509-4516.

[12] J.A.L. da Silva, J.J.R.F. da Silva, A.J.L. Pombeiro, Oxovanadium complexes in catalytic oxidations, Coordination Chemistry Reviews, 255 (2011) 2232-2248.

[13] T.A. Wencewicz, B. Yang, J.R. Rudloff, A.G. Oliver, M.J. Miller, N-O chemistry for antibiotics: Discovery of N-alkyl-N-(pyridin-2-yl) hydroxylamine scaffolds as selective antibacterial agents using nitroso diels-alder and ene chemistry, Journal of Medicinal Chemistry, 54 (2011) 6843-6858.

[14] G.M. Sheldrick, SHELXL-97: Program for the Refinement of Crystal Structure, in, University of Göttingen, Göttingen, Germany, 1997.

[15] J. Trnka, F.H. Blaikie, A. Logan, R.A.J. Smith, M.P. Murphy, Antioxidant properties of MitoTEMPOL and its hydroxylamine, Free Radical Research, 43 (2009) 4-12.

[16] R.R. Miller, G.A. Doss, R.A. Stearns, Identification of a hydroxylamine glucuronide metabolite of an oral hypoglycemic agent, Drug Metabolism and Disposition, 32 (2004) 178-185.

[17] J. Gun, I. Ekeltchik, O. Lev, R. Shelko, A. Melman, Bis-(hydroxyamino)triazines: Highly stable hydroxylamine-based ligands for iron(III) cations, Chemical Communications, (2005) 5319-5321.

[18] I. Ekeltchik, J. Gun, O. Lev, R. Shelkov, A. Melman, Bis(hydroxyamino)triazines: Versatile and high-affinity tridentate hydroxylamine ligands for selective iron(III) chelation, Dalton Transactions, 6 (2006) 1285-1293.

[19] D. Peri, J.S. Alexander, E.Y. Tshuva, A. Melman, Distinctive structural features of hydroxyamino-1,3,5-triazine ligands leading to enhanced hydrolytic stability of their titanium complexes, Dalton Transactions, (2006) 4169-4172.

[20] M. Shavit, D. Peri, A. Melman, E.Y. Tshuva, Antitumor reactivity of non-metallocene titanium complexes of oxygen-based ligands: Is ligand lability essential?, Journal of Biological Inorganic Chemistry, 12 (2007) 825-830.

[21] G. Melman, P. Vimal, A. Melman, Complementary dynamic assembly around an iron (III) cation, Inorganic Chemistry, 48 (2009) 8662-8664.

[22] F. Bou-Abdallah, J. McNally, X.X. Liu, A. Melman, Oxygen catalyzed mobilization of iron from ferritin by iron(iii) chelate ligands, Chemical Communications, 47 (2011) 731-733.

[23] A.D. Bond, W. Jones, Divalent complexes of 3-hydroxy-4-methyl-2(3H)-thiazolethione with Co-Zn: Synthesis, x-ray crystal structures and the structure-directing influence of C-H···S interactions, Journal of the Chemical Society, Dalton Transactions, (2001) 3045-3051.

[24] S. Abuskhuna, M. McCann, J. Briody, M. Devereux, K. Kavanagh, N. Kayal, V. McKee, Synthesis and structure of metal complexes containing zwitterionic N-hydroxyimidazole ligands, Polyhedron, 26 (2007) 4573-4580.

[25] M.D. Bachi, A. Melman, Stereocontrolled 5-Exo-Trig Cyclization of Imidoyl Radicals in the Synthesis of Substituted (Alkylthio)pyrrolines, Pyroglutamates, and Thiopyroglutamates, Journal of Organic Chemistry, 60 (1995) 6242-6244.

[26] S.A. Leaver, M. Palaniandavar, C.A. Kilner, M.A. Halcrow, A new synthesis of bis(2-{pyrid-2-yl}ethyl)amine (LH) from bis(2-{pyrid-2-yl}ethyl)hydroxylamine (LOH), and the copper-dependent reduction of LOH to LH, Dalton Transactions, (2003) 4224-4225.

[27] P. Bourosh, O. Bologa, V. Shafranski, E. Melnic, M. Gdanec, I. Bulhac, Cobalt(III) and nickel(II) complexes with 3-hydroxyamino-3-methylbutan-2-one thiosemicarbazone: Synthesis and structures, Russian Journal of Coordination Chemistry/Koordinatsionnaya Khimiya, 40 (2014) 891-903.

[28] S.V. Fokin, G.V. Romanenko, V.I. Ovcharenko, The first metal complex with a vic-dihydroxyamine and its oxidised derivative, Mendeleev Communications, 11 (2001) 127-128.

[29] P. KLEMCHUK, SUBSTITUTED HYDROXYLAMINE STABILIZERS, in: U.S.P.a.T.O.G. Patent (Ed.), US, 1972.

[30] A. Dey, J. Lakshmanan, The role of antioxidants and other agents in alleviating hyperglycemia mediated oxidative stress and injury in liver, Food and Function, 4 (2013) 1148-1184.

[31] M. Marí, A. Colell, A. Morales, C. Von Montfort, C. Garcia-Ruiz, J.C. Fernández-Checa, Redox control of liver function in health and disease, Antioxidants and Redox Signaling, 12 (2010) 1295-1331.

[32] S. Reuter, S.C. Gupta, M.M. Chaturvedi, B.B. Aggarwal, Oxidative stress, inflammation, and cancer: How are they linked?, Free Radical Biology and Medicine, 49 (2010) 1603-1616.

[33] Y.P. Lee, D.W. Kim, H.W. Kang, J.H. Hwang, H.J. Jeong, E.J. Sohn, M.J. Kim, E.H. Ahn, M.J. Shin, D.S. Kim, T.C. Kang, O.S. Kwon, S.W. Cho, J. Park, W.S. Eum, S.Y. Choi, PEP-1-heat shock protein 27 protects from neuronal damage in cells and in a Parkinson's disease mouse model, FEBS Journal, 279 (2012) 1929-1942.

[34] M.Y. Al-Maskari, M.I. Waly, A. Ali, Y.S. Al-Shuaibi, A. Ouhtit, Folate and vitamin B12 deficiency and hyperhomocysteinemia promote oxidative stress in adult type 2 diabetes, Nutrition, 28 (2012) e23-e26.

[35] S.H. Deo, J.P. Fisher, L.C. Vianna, A. Kim, A. Chockalingam, M.C. Zimmerman, I.H. Zucker, P.J. Fadel, Statin therapy lowers muscle sympathetic nerve activity and oxidative stress in patients with heart failure, American Journal of Physiology - Heart and Circulatory Physiology, 303 (2012) 377-385.

[36] V. Sánchez-Valle, N.C. Chávez-Tapia, M. Uribe, N. Méndez-Sánchez, Role of oxidative stress and molecular changes in liver fibrosis: A review, Current Medicinal Chemistry, 19 (2012) 4850-4860.

[37] P. Barberger-Gateau, J.C. Lambert, C. Féart, K. Pérès, K. Ritchie, J.F. Dartigues, A. Alpérovitch, From genetics to dietetics: The contribution of epidemiology to understanding Alzheimer's disease, in: Advances in Alzheimer's Disease, 2012, pp. 457-463.

[38] G.M. Sheldrick, SHELXS-97: Program for the Solution of Crystal Structure, in, University of Göttingen, Göttingen, Germany, 1997.

[39] L.J. Farrugia, J. Appl. Cryst., 32 (1999) 837.

[40] R.C. Clark, J.S. Reid, The analytical calculation of absorption in multifaceted crystals, Acta Crystallographica Section A, 51 (1995) 887-897.

[41] A.W. Addison, T.N. Rao, J. Reedijk, J. Van Rijn, G.C. Verschoor, Synthesis, structure, and spectroscopic properties of copper(II) compounds containing nitrogen-sulphur donor ligands; the crystal and molecular structure of aqua[1,7-bis(N-methylbenzimidazol-2′;-yl)-2,6-dithiaheptane]copper(II) perchlorate, Journal of the Chemical Society, Dalton Transactions, (1984) 1349-1356.

[42] J.E. Huheey, E.A. Keiter, R.L. Keiter, In Inorganic Chemistry: Principles of Structure and Reactivity, 4th ed., HarperCollins College Publishers, New York, 1993.

[43] H.N. Miras, D.J. Stone, E.J.L. McInnes, R.G. Raptis, P. Baran, G.I. Chilas, M.P. Sigalas, T.A. Kabanos, L. Cronin, Solution identification and solid state characterisation of a heterometallic polyoxometalate {Mo11V7}: [Mo VI11VV5VIV2O52(μ9-SO3)]7, Chemical Communications, (2008) 4703-4705.

[44] H.N. Miras, E.F. Wilson, L. Cronin, Unravelling the complexities of inorganic and supramolecular self-assembly in solution with electrospray and cryospray mass spectrometry, Chemical Communications, (2009) 1297-1311.

[45] E.F. Wilson, H.N. Miras, M.H. Rosnes, L. Cronin, Real-time observation of the self-assembly of hybrid polyoxometalates using mass spectrometry, Angewandte Chemie - International Edition, 50 (2011) 3720-3724.

[46] M.N. Corella-Ochoa, H.N. Miras, A. Kidd, D.L. Long, L. Cronin, Assembly of a family of mixed metal {Mo:V} polyoxometalates templated by TeO32-: {Mo12V12Te3}, {Mo12V12Te2} and {Mo17V8Te}, Chemical Communications, 47 (2011) 8799-8801.

[47] H.N. Miras, M. Sorus, J. Hawkett, D.O. Sells, E.J.L. McInnes, L. Cronin, Oscillatory template exchange in polyoxometalate capsules: A ligand-triggered, redox-powered, chemically damped oscillation, Journal of the American Chemical Society, 134 (2012) 6980-6983.

[48] H.N. Miras, D. Stone, D.L. Long, E.J.L. McInnes, P. Kögerler, L. Cronin, Exploring the structure and properties of transition metal templated {VM17(VO4)2} dawson-like capsules, Inorganic Chemistry, 50 (2011) 8384-8391.